10158 *Biochemistry* **2010,** *49,* 10158–10165
DOI: 10.1021/bi101462h

BIOCHEMISTRY
including biophysical chemistry & molecular biology
Article

Dissociation of the α-Subunit Calf-2 Domain and the β-Subunit I-EGF4 Domain in Integrin Activation and Signaling[†]

Wei Wang, Guanyuan Fu, and Bing-Hao Luo*

Department of Biological Sciences, 202 Life Sciences Building, Louisiana State University, Baton Rouge, Louisiana 70803, United States

Received September 9, 2010; Revised Manuscript Received October 28, 2010

ABSTRACT: Integrin conformational changes mediate integrin activation and signaling triggered by intracellular molecules or extracellular ligands. Even though it is known that αβ transmembrane domain separation is required for integrin signaling, it is still not clear how this signal is transmitted from the transmembrane domain through two long extracellular legs to the ligand-binding headpiece. This study addresses whether the separation of the membrane-proximal extracellular αβ legs is critical for integrin activation and outside-in signaling. Using a disulfide bond to restrict dissociation of the α-subunit Calf-2 domain and β-subunit I-EGF4 domain, we were able to abolish integrin inside-out activation and outside-in signaling. In contrast, disrupting the interface by introducing a glycosylation site into either subunit activated integrins for ligand binding through a global conformational change. Our results suggest that the interface of the Calf-2 domain and the I-EGF4 domain is critical for integrin bidirectional signaling.

Integrins are heterodimeric cell adhesion receptors that transmit signals bidirectionally across the plasma membrane. Together with other proteins, they mediate cell−cell and cell−extracellular matrix interactions and communication. As functionally important signaling molecules, they regulate a variety of cellular processes including growth, migration, differentiation, and survival. Integrins are normally inactive on the surface of the cell. When external agents stimulate cells, specific intracellular signals impinge on integrin cytoplasmic domains resulting in changes in structure and ligand-binding affinity in the integrin extracellular domain. In turn, binding of multimeric ligands triggers outside-in signaling, leading to several cellular processes including cell spreading and kinase activation. Thus, integrin activation and signaling are dependent on specific allosteric conformational changes in the integrin on the cell surface.

Integrin α and β subunits each have a large extracellular domain, a single transmembrane (TM) domain, and a short cytoplasmic domain (except the β4 subunit). The association of the α and β subunit TM/cytoplasmic tails is critical for maintaining integrins in the low-affinity state, whereas intracellular signals that destabilize αβ TM/cytoplasmic association result in integrin activation (*1*−*7*). Recently, the structure of the TM/cytoplasmic domains in the resting state was proposed based on Rosetta computational modeling and experimental data using intact integrins on mammalian cell surface (*8*). In this structure, the αIIb GXXXG motif and its β3 counterparts in the transmembrane domains associate with ridge-in-groove packing; the αIIb GFFKR motif and the β3 Lys716 in the cytoplasmic segments play a critical role in α/β association. Even though the role of two phenylalanines of the GFFKR in α/β association differs in the two latest NMR structures (*9*, *10*), mutagenesis studies showed that these two residues are important in integrin activation (*1*, *11*), and mutating them to other residues activates integrins, mimicking integrin inside-out activation (*3*, *8*). The structures of the monomeric α and β subunit TM/cytoplasmic domains have also been solved by NMR (*12*, *13*). These studies have shed light on the structural basis of integrin TM/cytoplasmic domain signaling across the plasma membrane (*14*). Binding of intracellular molecules such as talin (*15*) activates integrins, which dissociates the αβ TM/cytoplasmic domains and leads to a conformation with high affinity for ligands (*2*, *7*, *16*, *17*).

It has been well accepted that the conformational change of the integrin headpiece plays a critical role in affinity for binding ligands. During inside-out activation, the βI domain α7 helix assumes a crankshaft-like downward displacement, leading to structural rearrangement of the ligand-binding site, resulting in high affinity for ligands (*18*, *19*). However, the mechanism of how activation signals are transmitted from the TM domain through two long extracellular legs to the ligand-binding headpiece remains unclear. One model proposed that integrins assume high affinity for ligands even in the bent conformation, and overall conformational change is not critical for initial integrin activation but rather a postligand-binding event (*20*, *21*). By contrast, the other model, the "switchblade" model, proposed that upon inside-out activation the integrin extracellular domains rearrange through a "switchblade"-like movement to extend and assume high-affinity conformations for ligands (*22*). It suggests that this extension of extracellular integrin domains is critical for integrin activation and signaling, since it preferentially places the ligand-binding site away from the surface of the cell favoring ligand accessibility. At the same time, extension enables hybrid domain swing-out, thus pulling the βI domain α7 helix through the crankshaft-like displacement, converting the headpiece from the closed, low-affinity state to the open, high-affinity state (*23*). However, the role of two extracellular legs on integrin signaling

[†]We thank the American Heart Association (No. 10GRNT3960011) and the Louisiana Board of Regents (LEQSF(2009-12)-RD-A07) for financial support.

*To whom correspondence should be addressed. Phone: 225-578-7741. Fax: 225-578-2597. E-mail: luo@lsu.edu.

 Published on Web 11/01/2010

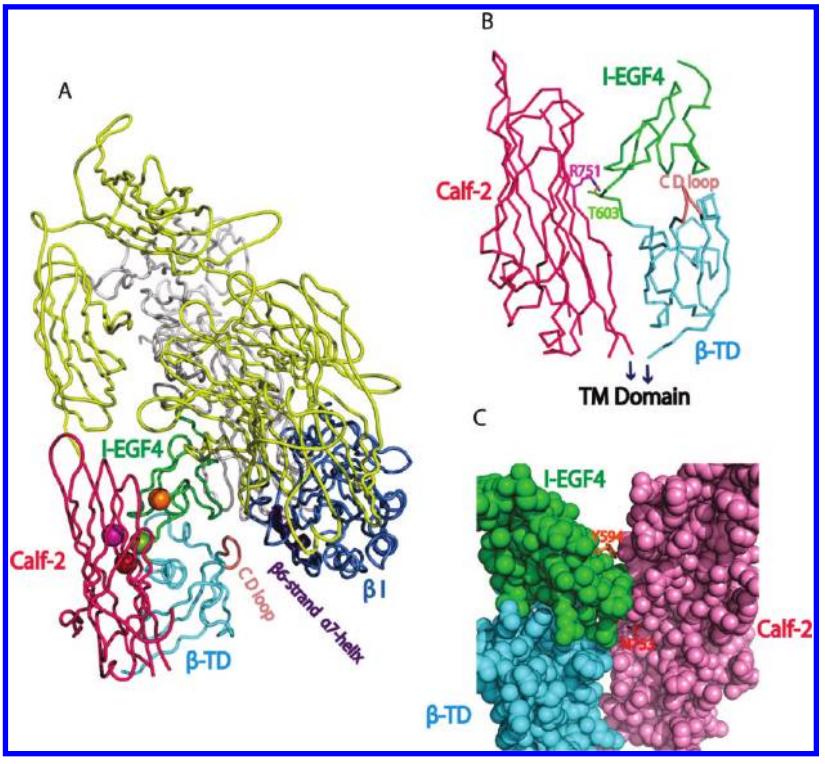

FIGURE 1: Mutations in the αIIbβ3 structure. The Calf-2 domain is in pink, the I-EGF4 domain is in green, and the βTD domain is in cyan. (A) The mutations are located one domain N-terminal to the βTD CD loop (in salmon). The ligand-binding βI domain is in marine, and the α7 helix is in purple. Mutated residues shown with spheres are residues R751 (magenta) and N753 (red) of αIIb and Y594 (orange) and T603 (split pea) of β3. (B) The αIIb_R751 (magenta) and β3_T603 (split pea) are close to each other, and mutating them to cysteines was expected to form a disulfide-linked heterodimer. (C) The αIIb N753 (red) and β3 Y594 (orange) are located at the interface, and introduction of a N-glycosylation site to these positions was predicted to disrupt αβ association.

remains elusive. Although the hybrid domain swing-out was observed by EM and crystal structures (*18*, *22*), conformational change of two lower legs is less defined. Patients with mutations in Calf-1 and Calf-2 domains of αIIbβ3 showed Glanzmann thrombasthenia (*24*), implying the significance of this region. Recently, a disulfide bond introduced into α5β1 Calf-2 and βTD[1] domain to restrict the leg separation blocked integrin extension and signaling (*25*).

In this paper, we tested the role of integrin lower leg separation on integrin activation and signaling by introducing mutations that either prevent or disrupt the interface between the α-subunit Calf-2 domain and β-subunit I-EGF4 domain (Figure 1). Our results showed that a disulfide bridge that prevents separation of this interface completely abolished integrin inside-out activation and outside-in signaling. In contrast, introduction of an N-glycan that disrupts this interface resulted in high-affinity conformations. The results indicate that the separation of the αβ legs is required for integrin bidirectional signaling.

MATERIALS AND METHODS

Plasmid Construction, Expression, and Immunoprecipitation. Plasmids with sequences for full-length human αIIb and β3 were subcloned into pEF/V5-HisA and pcDNA3.1/Myc-His (+), respectively (*22*). The αIIb mutants F992A/F993A (activating GAAKR mutant, denoted as α*), F755T, and α*R751C and the β3 mutants Y594N/D596T and T603C were made using site-directed mutagenesis with the QuikChange kit (Stratagene, La Jolla, CA). Constructs were transfected into HEK293T cells (American Type Culture Collection, Manassas, VA) using a FuGENE transfection kit (Roche Applied Science, Indianapolis, IN) according to the manufacturer's instructions. The expression levels of αIIb and β3 were detected by flow cytometry staining with the following monoclonal antibodies: AP3 (nonfunctional anti-β3 mAb; American Type Culture Collection), 7E3 (anti-β3 mAb), and 10E5 (anti-αIIb mAb; kindly provided by B. S. Coller, Rockefeller University, New York, NY). To characterize disulfide bond formation and glycosylation, transiently transfected cells were metabolically labeled with [^{35}S]cysteine/methionine as described (*3*). Lysates in 20 mM Tris-buffered saline, pH 7.4 (TBS), supplemented with 1 mM Ca^{2+}, 1% Triton X-100, and 0.1% Nonidet P-40 were immunoprecipitated with 1 μg of anti-β3 mAb AP3 and protein G−Sepharose at 4 °C for 1 h, eluted with 0.5% SDS. After the addition of 1% Nonidet P-40, the protein was treated with or without 500 units of PNGase F (New England BioLabs) at 37 °C for 1 h. Material was subjected to 7.5% nonreducing SDS−PAGE and fluorography (*3*).

Two-Color Ligand-Binding Assay on HEK293T Transfectants. Soluble binding of ligand-mimetic IgM PAC-1 (BD Biosciences, San Jose, CA) and Alexa Fluor 488-labeled human fibrinogen (Enzyme Research Laboratories, South Bend, IN) was determined as previously described (*26*). Briefly, transfected cells suspended in 20 mM HEPES-buffered saline, pH 7.4 (HBS), supplemented with 5.5 mM glucose and 1% bovine serum albumin were incubated on ice for 30 min with PAC-1 or Alexa Fluor 488-conjugated human fibrinogen in the presence of either 5 mM EDTA, 5 mM Ca^{2+}, 100 μM Ca^{2+}/1 mM Mn^{2+} plus 10 μg/mL

[1]Abbreviations: DIC, differential interference contrast; DTT, dithiothreitol; EM, electron microscopy; HPS, HEPES-buffered saline; LIBS, ligand-induced binding site; PBS, phosphate-buffered saline; βTD, β-tail domain; TBS, Tris-buffered saline; MFI, mean fluorescence intensity.

activating mAb PT25-2 (anti-αIIb, kindly provided by M. Handa, Keio University Hospital, Tokyo, Japan) (*27*) or 1 mM Mn^{2+} plus 10 μg/mL activating mAb LIBS-1 (anti-β3, kindly provided by M. H. Ginsberg, Scripps Research Institute, La Jolla, CA) (*28*). For PAC-1 binding, cells were washed and stained with FITC-conjugated anti-mouse IgM on ice for another 30 min before being subjected to flow cytometry. Cells were also stained in parallel with Cy3-conjugated anti-β3 mAb AP3. Binding activity is presented as the percentage of the mean fluorescence intensity (MFI) of PAC-1 or fibrinogen staining after background subtraction of the staining in the presence of EDTA, relative to the MFI of the AP3 staining.

Ligand-Induced Binding Site (*LIBS*) *Epitope Expression*. LIBS epitope expression was measured as previously described (*26*). Briefly, transfected cells suspended in HBS supplemented with 5.5 mM glucose and 1% bovine serum albumin were incubated with or without 50 μM GRGDSP peptide in the presence of 1 mM Mn^{2+} plus 10 μg/mL anti-LIBS antibody. After incubation on ice for 30 min, cells were washed and stained with FITC-labeled anti-mouse IgG on ice for 30 min. The stained cells were subjected to flow cytometry, and LIBS epitope expression was expressed as the percentage of MFI of anti-LIBS antibody relative to MFI of the conformation-independent anti-β3 mAb AP3.

Cell Adhesion Assays. Cell adhesion on immobilized human fibrinogen was assessed by the measurement of cellular lactate dehydrogenase (LDH) activity as previously described (*29*). Briefly, cells suspended in HBS supplemented with 5.5 mM glucose and 1% bovine serum albumin and 1 mM Ca^{2+} with or without 1 mM DTT were added into flat-bottom 12-well plates (1×10^5 cells/well) precoated with 20 μg/mL fibrinogen and blocked with 1% bovine serum albumin. After incubation at 37 °C for 1 h, wells were washed three times with HBS supplemented as indicated above. Remaining adherent cells were lysed with 1% Triton X-100, and LDH activity was assayed using the cytotoxicity detection kit (Roche Applied Science) according to the manufacturer's instructions. Cell adhesion was expressed as a percentage of bound cells relative to total input cells.

Cell Spreading and Microscopy. Glass-bottom six-well plates (MatTek Corp., Ashland, MA) were coated with 20 μg/mL human fibrinogen in phosphate-buffered saline at pH 7.4 (PBS) overnight at 4 °C and then blocked with 1% BSA at room temperature for 1 h. The transiently transfected HEK293T cells were detached with trypsin/EDTA, washed three times with DMEM, and seeded on fibrinogen-coated plates with or without 1 mM DTT. After incubation at 37 °C for 1 h, cells were washed three times with PBS and fixed with 3.7% formaldehyde in PBS at room temperature for 10 min for microscopy.

Differential interference contrast (DIC) imaging was conducted on a Leica TCS SP2 spectral confocal system coupled to a DM IRE2 inverted microscope with a 63× oil objective. For the quantification of cell spreading area, outlines of 100 randomly selected adherent cells were generated, and the number of pixels contained within each of these regions was measured using ImageJ software (Bethesda, Maryland).

RESULTS

Mutations of αIIbβ3 Extracellular Legs Stabilize or Disrupt αβ Leg Association. To test whether the conformational rearrangements of integrin lower legs are important, we designed mutations at the interface between the Calf-2 domain and the I-EGF4 domain (Figure 1A). To mimic integrin inside-out activation, site-directed mutagenesis was used to mutate two phenylalanine residues in the GFFKR motif of the αIIb cytoplasmic domain to alanines (αIIb_F992A/F993A/β3, denoted α*/β). Cysteine residues were introduced into the α*/β construct to test the effects of a disulfide-bridged mutant on integrin inside-out signaling (*3*). The distance between Cβ atoms of αIIb subunit Arg751 and β3 subunit Thr603 in the αIIbβ3 crystal structure is 4.1 Å (*19*). Therefore, cysteine residues introduced to replace these two residues (α*_R751C/β3_T603C, denoted α*751C/β603C) were expected to form a disulfide bond.

In addition to introducing this disulfide clasp to prevent the αβ dissociation, we also designed mutations to disrupt this interface to determine whether disrupting the αβ leg association affected ligand binding. N-Glycosylation sites were introduced on the αIIb subunit Calf-2 domain and on the β3 subunit I-EGF4 domain. In the crystal structure, the αIIb_N753 and β3_Y594 residues are at the interface between the Calf-2 and I-EGF4 domains (Figure 1C) and were predicted to be important for the αβ association. Therefore, introducing an N-glycan chain to either residue was expected to disrupt the αβ association. The following mutants were constructed to test this hypothesis: αIIb_F755T/β3 (denoted F755T/β, resulting in N-glycosylation of N753 in αIIb) and αIIb/β3_Y594N/D596T (denoted α/(Y594N/D596T), resulting in N-glycosylation of Y594N in β3).

Expression of Wild-Type and Mutant αIIbβ3 on HEK293T Cells. To determine the expression of wild-type and mutant αIIbβ3, wild-type and four mutated αIIb and β3 subunits were cotransfected into HEK293T cells and subjected to immunostaining flow cytometry (Figure 2). Two anti-β3 antibodies, AP3 and 7E3, which recognize the β3 I and hybrid domains, respectively, and one anti-αIIb antibody, 10E5, which recognizes the β-propeller domain, were used to monitor cell surface expression. Wild-type and mutant integrins bound to the three antibodies (Figure 2A), suggesting that they adopted a native conformation on the cell surface. To exclude the possible contribution of endogenous αV in HEK293T cell lines, β3 integrin alone was transfected into the cells, and none of these three antibodies bound (Figure 2A), suggesting that this cell line does not express endogenous αV integrin. Indeed, no αV expression was detected by using the anti-αV antibody LM609 (data not shown). When αV and β3 subunits were cotransfected into this cell line, the αV expression can be detected using LM609, suggesting that the antibody is functional.

Nonreducing SDS−PAGE of ^{35}S-labeled, immunoprecipitated receptors showed that in the activating mutant (Figure 2B, lane 2) the α* and the β3 subunits migrated in a similar pattern to the wild-type receptor (denoted α/β, Figure 2B, lane 1). In comparison, the receptors with the pair of cysteine mutants α*_R751C/β3_T603C formed a disulfide-linked receptor (Figure 2B, lane 3), and the efficiency of the disulfide-bond formation was close to 100%. The β3 subunit of β3-glycosylated mutant α/(Y594N/D596T) (Figure 2B, lane 4) migrated slightly slower than that of the wild type (Figure 2B, lane 1), whereas the αIIb subunit from this glycosylation mutant migrated in a similar pattern to the wild-type αIIb subunit, suggesting that there was an additional glycan chain added only to the β3 subunit. For the αIIb-glycosylation mutant F755T/β (Figure 2B, lane 5), the β3 subunit migrated in a similar pattern to the wild-type β3 (Figure 2B, lane 1), whereas the mutated αIIb subunit (Figure 2B, lane 5) migrated slightly slower than its wild-type counterpart (Figure 2B, lane 1), consistent with the presence of an additional glycan chain. Furthermore, these differences between the wild-type and glycosylation mutants

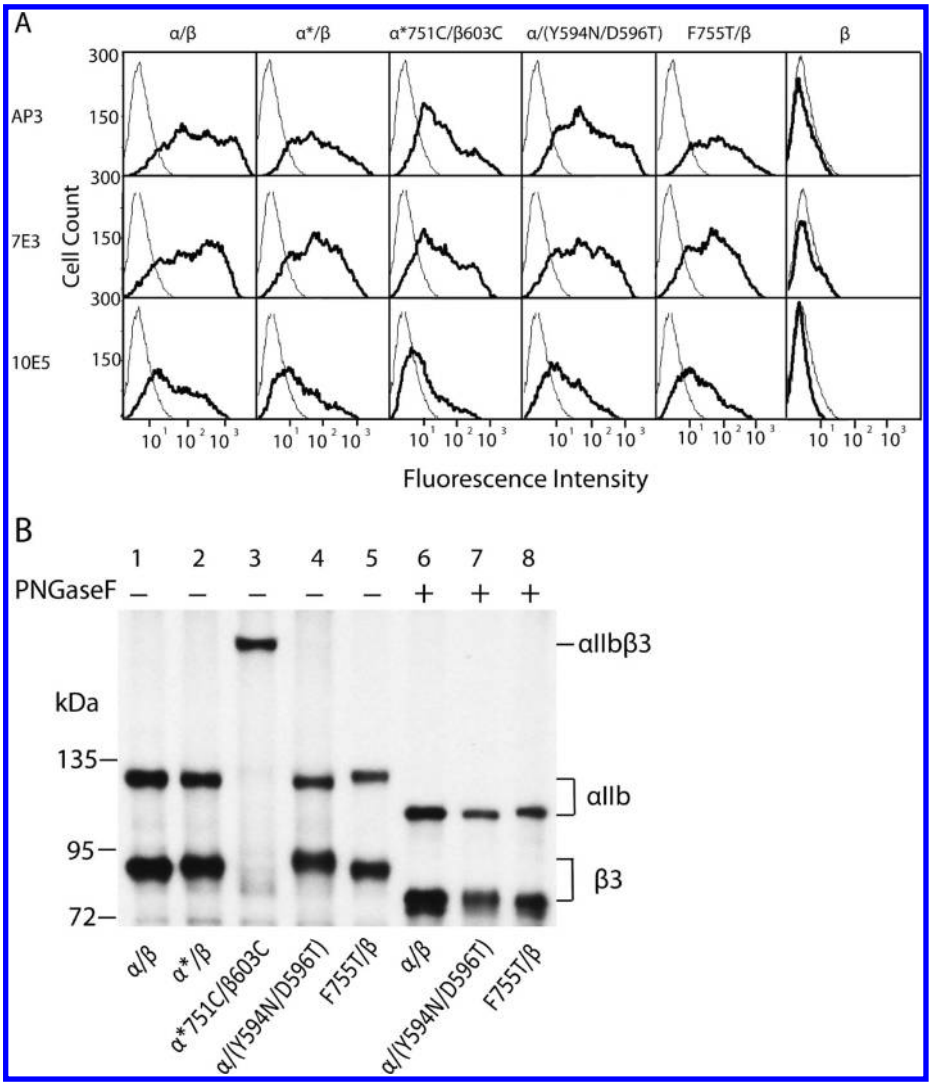

FIGURE 2: Expression and immunoprecipitation of wild-type and mutant αIIbβ3 integrins. (A) Immunofluorescent flow cytometry. HEK293T transfectants were labeled with AP3 (anti-β3), 7E3 (anti-β3), and 10E5 (anti-αIIb). Thick and thin lines show labeling of the αIIbβ3 transfectant and the mock transfectant, respectively. (B) Immunoprecipitation. Lysates from ^{35}S-labeled HEK293T cell transfectants were immunoprecipitated with mAb AP3. Precipitates were subjected to nonreducing 7.5% SDS−PAGE and fluorography.

disappeared on deglycosylation by PNGase F (Figure 2B, lanes 6−8), confirming the attachment of extra glycan chains.

Separation of the α-Subunit Calf-2 Domain and the β-Subunit I-EGF4 Domain Is Required for Integrin Inside-Out Signaling. Integrin inside-out signals are transmitted from the cytoplasmic/TM domains to the extracellular domains, leading to the conformational change of the ligand-binding headpiece, resulting in high-affinity ligand binding. To study the role of the separation of the Calf-2 domain and the I-EGF4 domain in integrin activation, two-color flow cytometry was used to determine the binding of the soluble ligand-mimetic antibody PAC-1 and fibrinogen to the wild-type and mutant receptors on the HEK293 cell surface (*4*). As shown in Figure 3A, the expression level of receptors was monitored by the Cy3-labeled anti-β3 antibody AP3. The fluorescence intensity was divided into four domains that represented specifically labeled receptors. The R1 and R2 domains contained cells designated as positive expressers. Ligand-binding affinity was monitored by the FITC-labeled PAC-1. Cells located in the R2 and R4 domains are those with high-affinity ligand binding. In the presence of Ca^{2+}, very few cells with the wild-type αIIbβ3 (α/β) were located in the R2 domain, and most positive expressers were in the R1 domain, indicating that wild-type αIIbβ3 bound very little ligand-mimetic PAC-1antibody. This is consistent with a low-affinity state under these physiological conditions. In the presence of Mn^{2+} and activating antibodies PT25-2, most positive expressers shifted to the R2 domain, indicating that wild-type αIIbβ3 bound PAC-1 with high affinity (Figure 3A). When the GFFKR motif of the αIIb was mutated to GAAKR, the mutant receptor (α*/β) bound PAC-1 with high affinity even in the presence of Ca^{2+}, since most positive expressers were located in the R2 domain (Figure 3A). The addition of the PT25-2 activating antibody did not change this pattern (Figure 3A), suggesting that the GAAKR mutation mimics integrin inside-out activation. When a disulfide bond was introduced to this activating mutant (α*751C/β603C), the ligand-binding affinity in the presence of Ca^{2+} was reversed, and a majority of the positive expressers were located in the R1 domain (Figure 3A), indicating that preventing separation of the αβ legs by a disulfide bond abolishes the integrin inside-out activation. In contrast, the two glycosylation mutants α/(Y594N/D596T) and F755T/β bound PAC-1 with high affinity in the presence of Ca^{2+} alone, with most positive expressers located in the R2 domain (Figure 3A). The addition of the PT25-2 activating antibody did not influence their ligand binding, suggesting

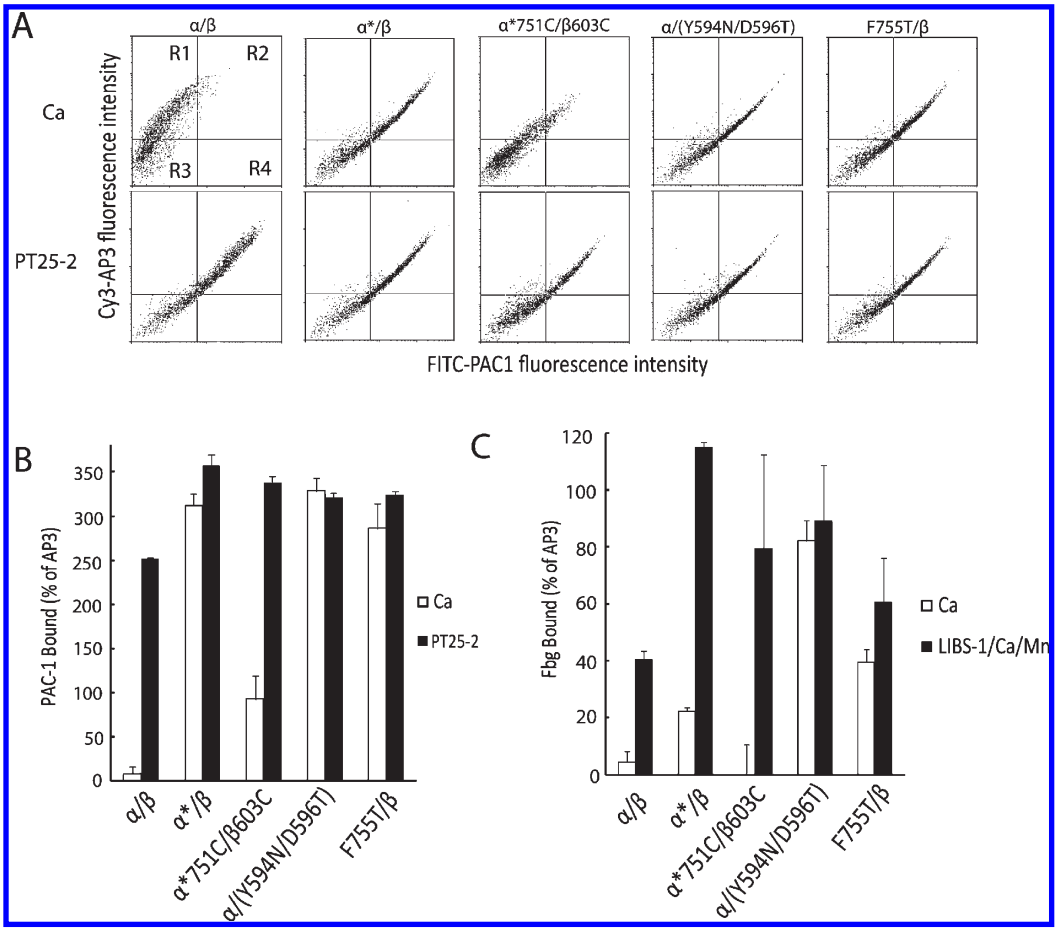

FIGURE 3: Ligand-binding activity of wild-type and mutant αIIbβ3 integrins. (A) Flow cytometry of dot plots. (B, C) Quantified soluble ligand-binding affinity. Cells were incubated with PAC-1 (A, B) in the presence of 5 mM Ca^{2+} or 10 μg/mL PT25-2 plus 1 mM Ca^{2+} or with FITC-fibrinogen (C) in the presence of 5 mM Ca^{2+} or 10 μg/mL LIBS1 plus 100 μM Ca^{2+} and 1 mM Mn^{2+} as indicated. Binding activities were determined by flow cytometry and expressed as described in Materials and Methods.

that these two mutants constitutively bound ligand with maximal affinity (Figure 3A).

Figure 3B quantifies these data by measuring the MFI of FITC-labeled PAC-1. The results confirmed that the wild-type receptor bound PAC-1 only in the presence of activating conditions, whereas the GAAKR mutant bound PAC-1 constitutively even in the presence of Ca^{2+} alone (Figure 3B). The disulfide-bonded receptor reversed the GAAKR-induced inside-out activation but did not abolish the activating antibody-induced ligand binding. When the N-glycan chain was introduced into the αβ interface of either subunit, receptors bound PAC-1 constitutively (Figure 3B). Soluble fibrinogen binding was also carried out, and similar results and conclusion were obtained (Figure 3C). Taken together, these experiments suggest that separation of the αβ lower legs is required and sufficient for integrin inside-out activation.

Disruption of the Interface between the α-Subunit Calf-2 Domain and the β-Subunit I-EGF4 Domain Causes a Global Integrin Conformational Change. Priming and ligand binding induce αIIbβ3 conformational changes that expose the LIBS epitopes. LIBS epitopes are at the interfaces between the headpiece and tailpiece and between the α and β legs so that they are buried in the bent conformation but exposed in the extended conformation (*22*, *30*). To investigate the conformational state of the αIIbβ3 mutants, binding of anti-β3 LIBS mAb LIBS1 (*31*) was analyzed. The LIBS1 bound poorly to wild-type αIIbβ3 in the presence of Ca^{2+} alone. The binding significantly increased when Mn^{2+} and the ligand-mimetic peptide GRGDSP were

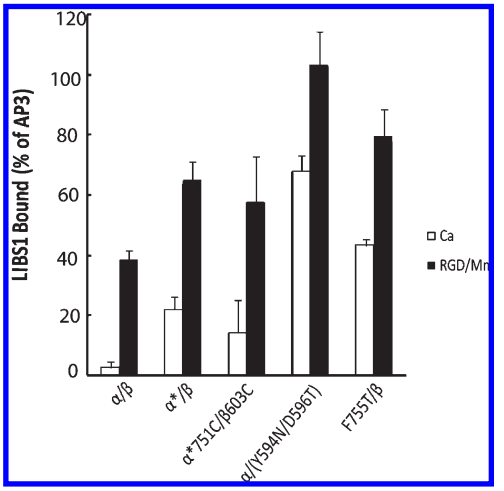

FIGURE 4: Exposure of the LIBS1 eptitope. Cells were stained with anti-LIBS antibody LIBS1 in the presence of 5 mM Ca^{2+} or 1 mM Mn^{2+} plus 50 μM RGD peptides (GRGDSP). LIBS epitope exposure was determined as the percentage of MFI of anti-LIBS1 antibody relative to nonfunctional anti-β3 mAb AP3. Error bars are standard deviation (SD).

added (Figure 4), suggesting that the ligand-mimetic peptide causes integrin conformational change. The GAAKR mutant (α*/β) bound LIBS1 better than the wild type in the presence of Ca^{2+} alone, suggesting that the mutation mimicking inside-out signaling changes the integrin global conformation. Addition of

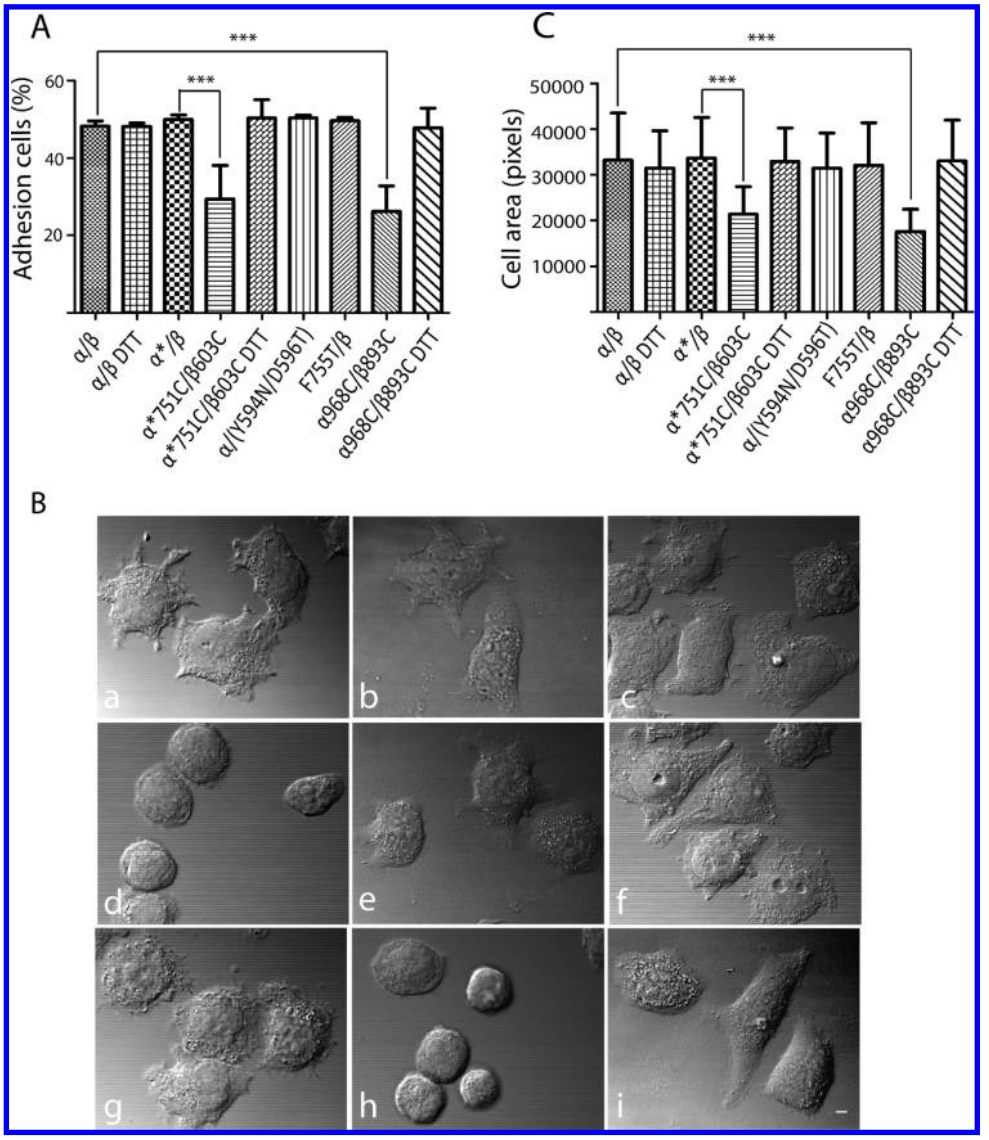

FIGURE 5: Cell adhesion and spreading. (A) Adhesion of HEK293T transfectants in the presence of 1 mM Ca^{2+} with or without DTT (1 mM) to surfaces coated with 20 μg/mL fibrinogen. The amount of bound cells was determined by measuring LDH activity as described in Materials and Methods. Data are representative of three independent experiments, each in triplicate. (B) DIC images of HEK293T transfectants after adhering to immobilized fibrinogen at 37 °C: a, α/β; b, α/β + DTT; c, α*/β; d, α*751C/β603C; e, α*751C β603C + DTT; f, α/(Y594N/D596T); g, F755T/β; h, α968C/β893C; i, α968C/β893C + DTT. The images are representatives of three independent experiments. Scale bar represents 10 μm. (C) Quantification of the areas of adhering/spreading cells as described in Materials and Methods. Error bars are SD; ***, $P < 0.001$.

Mn^{2+} and GRGDSP peptide further increased binding of the GAAKR mutant to LIBS1. In comparison, introducing the disulfide bond into this mutant (α*751C/β603C) slightly decreased LIBS1 binding in the presence of Ca^{2+} (Figure 4), suggesting that the disulfide bridge reverses the conformational change induced by inside-out activation. In contrast to the wild-type and the GAAKR mutant receptors, the two glycosylation mutants (α/Y594N/D596T and F755T/β) bound LIBS1 in the presence of Ca^{2+} (Figure 4), suggesting that separation of the two legs results in a global conformational change. Thus, this conformational change could explain their high affinity for ligand binding.

Separation of the α-Subunit Calf-2 Domain and the β-Subunit I-EGF4 Domain Is Crucial for Cell Adhesion and Spreading. We further determined how separation of the Calf-2 domain and the I-EGF4 domain affects outside-in signaling by assaying cell adhesion and spreading. HEK293T cells transiently transfected with wild-type and mutant αIIbβ3 were seeded on fibrinogen-precoated dish surfaces at 37 °C for 1 h. The amount of adherent cells was assessed by quantifying the cellular lactate dehydrogenase (LDH) activity. The results showed that in contrast to previous studies in CHO transfectants (*29*, *32*) all mutants with higher affinity for soluble ligands adhered to immobilized fibrinogen similarly to the wild-type cells. This suggests that the αIIbβ3 integrins in HEK293T cells are more active than similar integrins in CHO cells. In contrast, HEK293T cells transfected with a TM disulfide-bonded αIIbβ3 (α968C/β693C) showed much less adhesion than those with a wild-type receptor (Figure 5A). It is not surprising that the disulfide-bonded mutant (α*751C/β603C), which restricts separation of the αβ legs, exhibited less adhesion compared to the activating mutant (α*/β) (Figure 5A), since the adhesion strength is dependent not only on the affinity of the receptors but also on the spreading of the cells on the immobilized ligands. As shown below, the disulfide-bonded mutants had defective cell spreading, resulting in easier detachment of cells during washing. When these two disulfide-bonded mutants were treated with DTT, the cell adhesion ability was recovered to the similar level of the wild type with DTT.

To test if separation of the $\alpha\beta$ lower leg can affect cell spreading, HEK293T transient transfectants were coated on immobilized fibrinogen at 37 °C for 1 h, followed by fixation and microscopic analysis. Cells transfected with wild-type receptor demonstrated cell adhesion and cell spreading (Figure 5B). Previously, the TM disulfide-bonded αIIbβ3 (α968C/β693C) in CHO transfectants exhibited defective spreading, indicating that separation of the TM domains is required for integrin outside-in signaling (*29*). We confirmed that this disulfide-bonded mutant in HEK293T cells exhibited similar defective spreading on fibrinogen (Figure 5B), and even though some cell could adhere to the immobilized fibrinogen, they remained round and did not change size. The cell area was quantified and showed that the disulfide-bonded mutant had a significant decrease in adherent cell size comparing to that of the wild type (Figure 5C). Thus, this mutant was used as a control (Figure 5B,C). As we discussed in our previous paper (*29*), failure of outside-in signaling of the disulfide-bonded mutant was not likely due to the failure to bind ligands, since the mutant could bind soluble ligands with similar level as the wild type (Figure 3). The GAAKR mutant had little effect on cell spreading or on cell shape and size. By comparison, the disulfide-bonded mutant (α*751C/β603C) had defective spreading (Figure 5B,C). Most adherent cells remained round and stayed the same size (Figure 5B). We further determined the time course of the cell spreading of this mutant and the wild type. Our results showed that the wild type had full spreading within 30 min, and the mutant showed defective cell spreading even after 3 h (data not shown). To demonstrate that the defect in spreading was due to the disulfide linkage, we treated the cells with 1 mM DTT. Such treatment has shown to reduce the majority of engineered disulfides in the mutant receptor and rescued cell spreading of the TM linkage (Figure 5B,C) (*29*). Similarly, the DTT treatment of the disulfide-bonded integrin α*751C/β603C led to a rescue of cell spreading (Figure 5B,C). The effect of DTT treatment was unlikely due to the direct effect on ligand-binding affinity because DTT had little effect on wild-type cell adhesion and spreading (Figure 5). The quantitative adherent cell area of the disulfide-bonded mutant cells decreased by greater than 30% of that of the wild-type cells and of the GAAKR mutant cells. This suggests that separation of the α/β lower leg is crucial for cell spreading. HEK293T cells transfected with either glycosylation mutant could adhere to immobilized fibrinogen and demonstrated substantial spreading (Figure 5C). However, more glycosylation mutant cells than wild-type cells remained round (Figure 5B), suggesting that high-affinity mutants may have some defective effect on outside-in signaling probably due to their effect on cell detachment. Further research is required to determine the exact molecular mechanism of this defect.

DISCUSSION

When cells are activated, binding of intracellular molecules such as talin dissociates the $\alpha\beta$ TM/cytoplasmic domains and leads to integrin activation. The current study demonstrates that separation of the interface between the α-subunit Calf-2 domain and the β-subunit I-EGF4 domain is required for both integrin inside-out activation and outside-in signaling. Our study also suggests that the dissociation of the $\alpha\beta$ TM/cytoplasmic domains is coupled with the dissociation of the extracellular $\alpha\beta$ lower legs, specifically, the interface between the Calf-2 domain and the I-EGF4 domain. The mechanism by which this dissociation affects the conformational change of the upper legs and ligand-binding headpiece leading to high-affinity ligand binding remains to be determined.

When a disulfide bond was introduced to the Calf-2 and I-EGF4 interface, the mutant receptor could be activated from outside by external reagents such as Mn^{2+} and activating antibodies. In addition, LIBS epitope was exposed upon RGD binding, suggesting that the disulfide-bonded mutant could adopt an extended conformation. Similar results were obtained when a disulfide bond was introduced to the αIIbβ3 TM domain (*3*, *29*). This is probably because the β3 leg is highly flexible as suggested in the crystal structure (*19*). Interestingly, when a disulfide bond was introduced to the $\alpha5\beta1$ Calf-2 and βTD interface, the mutant $\alpha5\beta1$ failed to be extended(*25*). The discrepancy may be due to the varied role of different interfaces on integrin activation or due to different integrin families. While the β3 integrins must respond rapidly to environment (*33*), changing their conformation within seconds from their default low-affinity state to high-affinity state, the β1 integrins do not require a rigid control of their affinity (*25*).

It is still controversial whether integrin extension is required for integrin activation and signaling (*17*, *34*−*40*). In the present study, the inside-out activation by GAAKR mutation only slightly exposed the LIBS1 epitope (Figure 4), and addition of a ligand-mimetic peptide further exposed the epitope, suggesting that this inside-out activation does not induce full extension of all integrin molecules. Inside-out activating signals may act by shifting the equilibrium, but not stabilizing integrins in the fully extended state, which represents an extreme conformation. However, this equilibrium shift is sufficient to initiate ligand binding. Regardless of the extent of integrin extension, separation of the TM/cytoplasmic tails (*3*, *16*, *17*, *41*) and dissociation of the lower $\alpha\beta$ legs as observed in the present and previous (*25*) studies are required for the transmission of the inside-out signals to the ligand-binding headpiece. This observation is consistent with a previous crystallography study of the complete ectodomain of integrin αIIbβ3 (*19*), which suggested that breathing motions at the lower α and β legs might be a pathway for integrin extension, and this motion shifts equilibrium toward more extended and higher affinity states. EM studies of three integrin families showed that the legs of the extended integrins are often crossed at the α and β genu region (*17*, *19*, *22*, *37*), suggesting that more structural assessments are needed to determine how signals are conveyed between the headpiece and the lower legs.

Outside-in signaling is induced by binding of integrins to multimeric ligands, which results in integrin conformational change and clustering, both of which are critical for signaling. A number of studies showed that binding of ligands or ligand-mimetic peptides stabilizes integrins in the more extended conformation (*19*, *22*, *37*, *38*). However, it is not known whether integrins assume a fully extended conformation on the cell surface upon ligand binding in the physiological conditions. It is evident from the present study and previous publications that dissociation of the lower $\alpha\beta$ legs and the TM/cytoplasmic tails is required for this signal transduction.

In conclusion, our study strongly suggests that a global conformational change is required to transmit integrin inside-out activation. Introduction of a glycan chain to dissociate the $\alpha\beta$ lower legs leads to both a high-affinity ligand-binding state and a global conformational change, whereas introduction of a disulfide bond to restrict the dissociation abolishes both inside-out and outside-in signaling. Thus, this interface lies within the critical pathway of integrin bidirectional signaling.

REFERENCES

1. Hughes, P. E., Diaz-Gonzalez, F., Leong, L., Wu, C., McDonald, J. A., Shattil, S. J., and Ginsberg, M. H. (1996) Breaking the integrin hinge. *J. Biol. Chem. 271*, 6571–6574.
2. Vinogradova, O., Velyvis, A., Velyviene, A., Hu, B., Haas, T. A., Plow, E. F., and Qin, J. (2002) A structural mechanism of integrin $a_{IIb}b_3$ "inside-out" activation as regulated by its cytoplasmic face. *Cell 110*, 587–597.
3. Luo, B. H., Springer, T. A., and Takagi, J. (2004) A specific interface between integrin transmembrane helices and affinity for ligand. *PLoS Biol. 2*, 776–786.
4. Luo, B. H., Carman, C. V., Takagi, J., and Springer, T. A. (2005) Disrupting integrin transmembrane domain heterodimerization increases ligand binding affinity, not valency or clustering. *Proc. Natl. Acad. Sci. U.S.A. 102*, 3679–3684.
5. Li, W., Metcalf, D. G., Gorelik, R., Li, R., Mitra, N., Nanda, V., Law, P. B., Lear, J. D., Degrado, W. F., and Bennett, J. S. (2005) A push-pull mechanism for regulating integrin function. *Proc. Natl. Acad. Sci. U.S.A. 102*, 1424–1429.
6. Partridge, A. W., Liu, S., Kim, S., Bowie, J. U., and Ginsberg, M. H. (2005) Transmembrane domain packing stabilizes integrin aIIbb3 in the low affinity state. *J. Biol. Chem. 280*, 7294–7200.
7. Kim, M., Carman, C. V., and Springer, T. A. (2003) Bidirectional transmembrane signaling by cytoplasmic domain separation in integrins. *Science 301*, 1720–1725.
8. Zhu, J., Luo, B. H., Barth, P., Schonbrun, J., Baker, D., and Springer, T. A. (2009) The structure of a receptor with two associating transmembrane domains on the cell surface: integrin alphaIIbbeta3. *Mol. Cell 34*, 234–249.
9. Lau, T. L., Kim, C., Ginsberg, M. H., and Ulmer, T. S. (2009) The structure of the integrin alphaIIbbeta3 transmembrane complex explains integrin transmembrane signalling. *EMBO J. 28*, 1351–1361.
10. Yang, J, Ma, Y. Q., Page, R. C., Misra, S., Plow, E. F., and Qin, J. (2009) Structure of an integrin alphaIIb beta3 transmembrane-cytoplasmic heterocomplex provides insight into integrin activation. *Proc. Natl. Acad. Sci. U.S.A. 106*, 17729–17734.
11. O'Toole, T. E., Katagiri, Y., Faull, R. J., Peter, K., Tamura, R., Quaranta, V., Loftus, J. C., Shattil, S. J., and Ginsberg, M. H. (1994) Integrin cytoplasmic domains mediate inside-out signal transduction. *J. Cell Biol. 124*, 1047–1059.
12. Lau, T. L., Partridge, A. W., Ginsberg, M. H., and Ulmer, T. S. (2008) Structure of the integrin beta3 transmembrane segment in phospholipid bicelles and detergent micelles. *Biochemistry 47*, 4008–4016.
13. Lau, T. L., Dua, V., and Ulmer, T. S. (2008) Structure of the integrin alphaIIb transmembrane segment. *J. Biol. Chem. 283*, 16162–16168.
14. Wang, W, and Luo, B. H. (2010) Structural basis of integrin transmembrane activation. *J. Cell. Biochem. 109*, 447–452.
15. Wegener, K. L., Partridge, A. W., Han, J., Pickford, A. R., Liddington, R. C., Ginsberg, M. H., and Campbell, I. D. (2007) Structural basis of integrin activation by talin. *Cell 128*, 171–182.
16. Anthis, N. J., Wegener, K. L., Ye, F., Kim, C., Goult, B. T., Lowe, E. D., Vakonakis, I., Bate, N., Critchley, D. R., Ginsberg, M. H., and Campbell, I. D. (2009) The structure of an integrin/talin complex reveals the basis of inside-out signal transduction. *EMBO J. 28*, 3623–3632.
17. Ye, F., Hu, G., Taylor, D., Ratnikov, B., Bobkov, A. A., McLean, M. A., Sligar, S. G., Taylor, K. A., and Ginsberg, M. H. (2010) Recreation of the terminal events in physiological integrin activation. *J. Cell Biol. 188*, 157–173.
18. Xiao, T., Takagi, J., Wang, J.-h., Coller, B. S., and Springer, T. A. (2004) Structural basis for allostery in integrins and binding of fibrinogen-mimetic therapeutics. *Nature 432*, 59–67.
19. Zhu, J., Luo, B. H., Xiao, T., Zhang, C., Nishida, N., and Springer, T. A. (2008) Structure of a complete integrin ectodomain in a physiologic resting state and activation and deactivation by applied forces. *Mol. Cell 32*, 849–861.
20. Xiong, J. P., Stehle, T., Goodman, S. L., and Arnaout, M. A. (2003) New insights into the structural basis of integrin activation. *Blood 102*, 1155–1159.
21. Arnaout, M. A., Mahalingam, B., and Xiong, J. P. (2005) Integrin structure, allostery, and bidirectional signaling. *Annu. Rev. Cell Dev. Biol. 21*, 381–410.
22. Takagi, J., Petre, B. M., Walz, T., and Springer, T. A. (2002) Global conformational rearrangements in integrin extracellular domains in outside-in and inside-out signaling. *Cell 110*, 599–611.
23. Luo, B. H., and Springer, T. A. (2006) Integrin structures and conformational signaling. *Curr. Opin. Cell Biol. 18*, 579–586.
24. Rosenberg, N., Yatuv, R., Sobolev, V., Peretz, H., Zivelin, A., and Seligsohn, U. (2003) Major mutations in calf-1 and calf-2 domains of glycoprotein IIb in patients with Glanzmann thrombasthenia enable GPIIb/IIIa complex formation but impair its transport from the endoplasmic reticulum to the Golgi apparatus. *Blood 101*, 4808–4815.
25. Askari, J. A., Tynan, C. J., Webb, S. E., Martin-Fernandez, M. L., Ballestrem, C., and Humphries, M. J. (2010) Focal adhesions are sites of integrin extension. *J. Cell Biol. 188*, 891–903.
26. Luo, B. H., Springer, T. A., and Takagi, J. (2003) Stabilizing the open conformation of the integrin headpiece with a glycan wedge increases affinity for ligand. *Proc. Natl. Acad. Sci. U.S.A. 100*, 2403–2408.
27. Tokuhira, M., Handa, M., Kamata, T., Oda, A., Katayama, M., Tomiyama, Y., Murata, M., Kawai, Y., Watanabe, K., and Ikeda, Y. (1996) A novel regulatory epitope defined by a murine monoclonal antibody to the platelet GPIIb-IIIa complex (αIIbβ3 integrin). *Thromb. Haemostasis 76*, 1038–1046.
28. Frelinger, A. L., Cohen, I., Plow, E. F., Smith, M. A., Roberts, J., Lam, S. C. T., and Ginsberg, M. H. (1990) Selective inhibition of integrin function by antibodies specific for ligand-occupied receptor conformers. *J. Biol. Chem. 265*, 6346–6352.
29. Zhu, J., Carman, C. V., Kim, M., Shimaoka, M., Springer, T. A., and Luo, B. H. (2007) Requirement of α and β subunit transmembrane helix separation for integrin outside-in signaling. *Blood 110*, 2475–2483.
30. Beglova, N., Blacklow, S. C., Takagi, J., and Springer, T. A. (2002) Cysteine-rich module structure reveals a fulcrum for integrin rearrangement upon activation. *Nat. Struct. Biol. 9*, 282–287.
31. Du, X., Gu, M., Weisel, J. W., Nagaswami, C., Bennett, J. S., Bowditch, R., and Ginsberg, M. H. (1993) Long range propagation of conformational changes in integrin $\alpha_{IIb}\beta_3$. *J. Biol. Chem. 268*, 23087–23092.
32. Luo, B.-H., Takagi, J., and Springer, T. A. (2004) Locking the β3 integrin I-like domain into high and low affinity conformations with disulfides. *J. Biol. Chem. 279*, 10215–10221.
33. Shattil, S. J., Kashiwagi, H., and Pampori, N. (1998) Integrin signaling: the platelet paradigm. *Blood 91*, 2645–2657.
34. Ye, F., Liu, J., Winkler, H., and Taylor, K. A. (2008) Integrin alpha IIb beta 3 in a membrane environment remains the same height after Mn^{2+} activation when observed by cryoelectron tomography. *J. Mol. Biol. 378*, 976–986.
35. Kamata, T., Handa, M., Sato, Y., Ikeda, Y., and Aiso, S. (2005) Membrane-proximal α/β stalk interactions differentially regulate integrin activation. *J. Biol. Chem. 280*, 24775–24783.
36. Xiong, J. P., Mahalingham, B., Alonso, J. L., Borrelli, L. A., Rui, X., Anand, S., Hyman, B. T., Rysiok, T., Müller-Pompalla, D., Goodman, S. L., and Arnaout, M. A. (2009) Crystal structure of the complete integrin alphaVbeta3 ectodomain plus an alpha/beta transmembrane fragment. *J. Cell Biol. 186*, 589–600.
37. Nishida, N., Xie, C., Shimaoka, M., Cheng, Y., Walz, T., and Springer, T. A. (2006) Activation of leukocyte β2 integrins by conversion from bent to extended conformations. *Immunity 25*, 583–594.
38. Xie, C., Zhu, J., Chen, X., Mi, L., Nishida, N., and Springer, T. A. (2010) Structure of an integrin with an alphaI domain, complement receptor type 4. *EMBO J. 29*, 666–679.
39. Chigaev, A., Buranda, T., Dwyer, D. C., Prossnitz, E. R., and Sklar, L. A. (2003) FRET detection of cellular α4-integrin conformational activation. *Biophys. J. 85*, 3951–3962.
40. Blue, R., Li, J., Steinberger, J., Murcia, M., Filizola, M., and Coller, B. S. (2010) Effects of limiting extension at the alphaIIb genu on ligand binding to integrin alphaIIbbeta3. *J. Biol. Chem. 285*, 17604–17613.
41. Anthis, N. J., Haling, J. R., Oxley, C. L., Memo, M., Wegener, K. L., Lim, C. J., Ginsberg, M. H., and Campbell, I. D. (2009) Beta integrin tyrosine phosphorylation is a conserved mechanism for regulating talin-induced integrin activation. *J. Biol. Chem. 284*, 36700–36710.